Inorganic Chemistry

ARTICLE

pubs.acs.org/IC

TSQ (6-Methoxy-8-*p*-Toluenesulfonamido-Quinoline), a Common Fluorescent Sensor for Cellular Zinc, Images Zinc Proteins

Jeffrey W. Meeusen,[†,§] Henry Tomasiewicz,[‡] Andrew Nowakowski,[†] and David H. Petering*[,†]

[†]Department of Chemistry and Biochemistry, and [‡]National Institute of Environmental Health Science Children's Environmental Health Sciences Core Center, University of Wisconsin-Milwaukee, Milwaukee, Wisconsin 53201, United States

Supporting Information

ABSTRACT: Zn^{2+} is a necessary cofactor for thousands of mammalian proteins. Research has suggested that transient fluxes of cellular Zn^{2+} are also involved in processes such as apoptosis. Observations of Zn^{2+} trafficking have been collected using Zn^{2+} responsive fluorescent dyes. A commonly used Zn^{2+} fluorophore is 6-methoxy-8-*p*-toluenesulfonamido-quinoline (TSQ). The chemical species responsible for TSQ's observed fluorescence in resting or activated cells have not been characterized. Parallel fluorescence microscopy and spectrofluorometry of LLC-PK_1 cells incubated with TSQ demonstrated punctate staining that concentrated around the nucleus and was characterized by an emission maximum near 470 nm. Addition of cell permeable Zn-pyrithione resulted in greatly increased, diffuse fluorescence that shifted the emission peak to 490 nm, indicative of the formation of $Zn(TSQ)_2$. TPEN (*N*,*N*,*N*′*N*′-tetrakis(-)[2-pyridylmethyl]-ethylenediamine), a cell permeant Zn^{2+} chelator, largely quenched TSQ fluorescence returning the residual fluorescence to the 470 nm emission maximum. Gel filtration chromatography of cell supernatant from LLC-PK_1 cells treated with TSQ revealed that TSQ fluorescence (470 nm emission) eluted with the proteome fractions. Similarly, addition of TSQ to proteome prior to chromatography resulted in 470 nm fluorescence emission that was not observed in smaller molecular weight fractions. It is hypothesized that Zn-TSQ fluorescence, blue-shifted from the 490 nm emission maximum of $Zn(TSQ)_2$, results from ternary complex, TSQ-Zn-protein formation. As an example, Zn-carbonic anhydrase formed a ternary adduct with TSQ characterized by a fluorescence emission maximum of 470 nm and a dissociation constant of 1.55×10^{-7} M. Quantification of TSQ-Zn-proteome fluorescence indicated that approximately 8% of cellular Zn^{2+} was imaged by TSQ. These results were generalized to other cell types and model Zn-proteins.

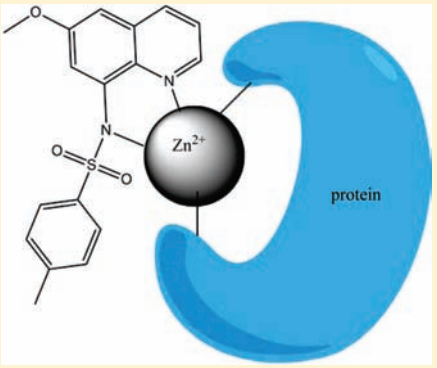

INTRODUCTION

Zn^{2+} has been identified as an integral constituent in thousands of proteins through mammalian genomic analysis.[1] These include hundreds of enzymes and as many as one thousand zinc-finger eukaryotic transcription factors.[1,2] Beyond its role as a metalloprotein cofactor, studies imply that Zn^{2+} participates directly in dynamic cellular signaling processes such as synaptic chemical transmission and endocrine signaling.[3,4]

Support for such activities has emerged from the use of fluorescent probes for Zn^{2+}.[5−7] For example, results with fluorescent probes that detected presumed fluctuations in chelatable Zn^{2+} have led to the hypothesis that Zn^{2+} ion is a chemical messenger in neural synapses.[8,9] An increase in Zn^{2+} sensor signal in several brain injury models has suggested that chelatable Zn^{2+} accumulation plays a causal role in neurodegeneration.[10−12] Exposing pulmonary endothelial cells to nitric oxide or lipopolysaccharide increases a Zn^{2+} sensor signal, implying that Zn^{2+} release is involved in cellular signaling pathways.[13−15]

Fluorescence enhancement has been interpreted as evidence of free, loosely bound, accessible, or chelatable metal ions that are available to react with sensors.[16] It has been argued that little if any unbound transition metal ions exist within the ligand rich environment of cells.[17] Nevertheless, the extent of availability of metal ions for reaction with sensors surely depends on cell type and, probably, other specific factors. In this broad context the appearance of fluorescence likely represents the reaction of the sensor (S) with bound forms of M^{n+}, such as metalloproteins (M-protein):

$$\text{M-protein} + \text{S} \rightleftharpoons \text{M-S} + \text{apo-protein} \quad (1)$$

The identification of such reaction sites is key to understanding what pools of metal ion are imaged by the fluorescent probe.[18] In the absence of biochemical studies that reveal the sources of M^{n+} reacting with S, the linkage between fluorescence enhancement and its chemical origins cannot be established.

Commonly used Zn^{2+} sensors are the quinoline-based fluorophores TSQ (6-methoxy-8-*p*-toluenesulfonamido-quinoline) and its relatives, Zinquin (ethyl[2-methyl-8-*p*-toluenesulfonamido-6-quinolyloxy]acetate) and TFL (Figure 1).[8−12,18−26] TSQ and its related fluorophores are bidentate ligands, utilizing quinoline and sulfonamide nitrogens to coordinate Zn^{2+}.[21,27] Hence,

Received: March 8, 2011
Published: July 20, 2011

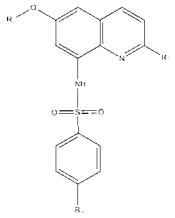

	R_1	R_2	R_3
TSQ	H	CH_3	CH_3
2-Me-TSQ	CH_3	CH_3	CH_3
Zinquin	CH_3	CH_2COOH	CH_3
TFL	CH_3	CH_3	COOH

Figure 1. Chemical structure of TSQ and several analogues which have been widely used in Zn^{2+} sensing fluorescence experiments.

they bind Zn^{2+} in a 2:1 ligand to metal ratio as in reaction 2.

$$2TSQ + Zn^{2+} \rightleftharpoons Zn(TSQ)_2 \quad (2)$$

Zn^{2+} binding is accompanied by the appearance of an intense fluorescence emission spectrum (excitation maximum: 360 nm, emission maximum: 490 nm).

Bidentate ligand binding opens the possibility that a single Zn^{2+} ion may bind one of these sensor molecules while coordinated to a second, nonsensor ligand. A recent study demonstrated that Zinquin does form ternary complexes with a number of Zn^{2+} bound multidentate ligand frameworks that permit additional ligand coordination.[19] These adducts display emission spectra similar to ZnL_2 (L = TSQ, Zinquin). However, such ternary complexes are distinguishable from ZnL_2 by their blue-shifted emission spectrum.[19] Although these unique spectra are readily observed by spectrofluorometry, conventional fluorescence microscopy that utilizes DAPI/FITC filters to define fluorescence emission wavelength windows does not readily distinguish between $Zn(TSQ)_2$ and ternary complexes in cells. This lack of detailed spectrofluorometric analysis of cells treated with TSQ or Zinquin led us to consider the possibility that the fluorescence observed in intracellular studies may arise from the coordination of these sensors to Zn^{2+} already bound to biological ligands such as proteins.

$$TSQ + Zn\text{-Protein} \rightleftharpoons TSQ\bullet Zn\text{-Protein} \quad (3)$$

If correct, these Zn^{2+} responsive fluorophores image Zn-proteins not Zn^{2+} in resting cells. This paper begins a study aimed at making this connection with the most commonly used class of Zn^{2+} fluorescent probes, toluenesulfonamido−quinoline compounds.

EXPERIMENTAL SECTION

Cell Culture. Cell lines except CCRF-CEM were purchased from the American Tissue Culture Company. The media for all these cell lines were supplemented with 50 000 units/L Penicillin G and 50 mg/L streptomycin. LLC-PK_1 cells were grown in Medium 199 with HEPES modification (Sigma) supplemented with 4% fetal calf serum. Flasks were incubated under 5% CO_2 at 37 °C and the medium was changed every 48 h. Cultures were subdivided by trypsin/EDTA treatment every 5−7 days. $ZnCl_2$ (40 μM) was added to the medium 24 h prior to isolation of cells in order to induce the synthesis of cytosolic metallothionein. Exposures of these and other cells to TSQ, pyrithione (PYR), or *N*,*N*,*N*′,*N*′-tetrakis(2-pyridylmethyl) ethylenediamine (TPEN) were conducted at concentrations that did not affect viability as measured by the 3(4,5-dimethyl-2-thiazoyl)-2,5-diphenyl-2H-tetrazolium, bromide (MTT) assay.

TE-671 human muscle meduloblastoma cells were grown in Dulbecco's Minimal Essential Growth-Low Glucose (Sigma) medium supplemented with 5% FCS. U-87 MG human brain glioblastoma cells were cultured in Eagles' Minimum Essential Media (Sigma) supplemented with 5% FCS. C6 rat glioma and A549 human lung adenocarcinoma cells were grown in Ham's F-12 Nutrient Mixture-Kaighn's Modification (Sigma) medium. C6 cells were supplemented with 15% horse serum and 2.5% FCS; A549 cells were supplemented with 10% FCS. TE-671 and U-87 MG cells were cultured in a 6% CO_2 atmosphere, and C6 and A549 cells were cultured in 5% CO_2. All cells were incubated at 37 °C.

CCRF-CEM human lymphocytic leukemia cells were grown in suspension (2×10^5 to 1×10^6 cells/mL) in RPMI 1640 (Sigma) medium supplemented with 10% FCS. They were incubated in the presence of 6% CO_2 at 37 °C. Media for all cell cultures was changed every 48−72 h until confluence or maximum concentration was reached, at which time cells were harvested for experiments.

Cell Suspensions. Mixed neuron/astrocyte cell suspension of the cortex region and suspension of the rest of the brain were prepared from fetal mice after 15−16 days of gestation. Pregnant mice were anesthetized with isoflurane and subsequently euthanized. Brain tissues from 7−8 fetal mice were isolated and placed into 3 mL of Eagles' Minimum Essential Media. Cell suspensions were washed 3 times in Dulbecco's phosphate-buffered saline (DPBS, Sigma) using a disposable pipet to fragment the fragile tissue before experiments were performed.

Microscopic Imaging. Cells were grown on 22-mm Round No. 1 German glass coverslips coated with rat tail collagen (BD BioScience). When cells reached desired confluence, they were rinsed three times with DPBS (Sigma) and stained for 30 min in the incubator using a solution of 30 μM TSQ in DPBS. After the stained cells were rinsed three times with DPBS, the coverslip was mounted on an Olympus IX-70 inverted fluorescence microscope equipped with a mercury lamp. A custom filter cube with a 360 ± 40 nm bandpass excitation filter, a 500 ± 40 nm emission filter, and a 400-nm dichroic mirror were used in all fluorescent micrographs. All images were recorded using an Olympus 60x UPlanFL oil immersion objective lens.

Toxicity of Reagents. The toxicity of TSQ, PYR, and TPEN ligands was studied by dose response experiments. A suspension of 5×10^4 cells/mL supplemented with 5% FCS was prepared and aliquots of 1 mL were added into each well of a 24-well plate. Several concentrations of ligand, including no dose, were used. The plates were incubated for 1 h or 24 h and the ligand cytotoxicity was assessed by the MTT assay.

In this assay, the viability of the cells is assessed by their ability to convert the tetrazolium salt MTT to formazan.[28] This reaction is carried out by the mitochondrial electron pathway and is therefore an indicator of healthy cellular ATP production capability. MTT was prepared in saline at a concentration of 5 mM and syringe filtered to sterilize and remove insoluble particles. Then, 100 μL was added to each well of the 24-well plate and the 1.1-mL cultures were incubated for 2 h at 37 °C. Subsequently, the media was removed from the wells and 1 mL of acidified (0.04 N HCl) isopropanol was added to each well to dissolve the dark blue formazan crystals. The absorbance (A) at 570 and 630 nm was measured and the difference of $A_{570} - A_{630}$ was recorded and calculated as a relative measure of viability when normalized to zero exposure samples.

Fluorescence Spectroscopy of Whole Cells. Cells were grown in 35-mm culture plates and rinsed three times with 2 mL of DPBS to remove any extracellular Zn^{2+} prior to being stained for 30 min with 30 μM TSQ in DPBS. After exposure to TSQ, cells were again rinsed three times with 2 mL of DPBS. Then, cells were suspended in 1 mL of DPBS by gentle scraping with a rubber policeman. Cell suspensions were added to a fluorescence cuvette. The emission spectrum was recorded between 400 and 600 nm with a Hitachi F4500 spectrofluorometer using an excitation wavelength of 360 nm.

Quantitation of Cellular TSQ. The fluorescence intensity (F) of a suspension of cells stained with TSQ was recorded. To determine the total amount of TSQ in solution, 50 μM PYR and 100 μM $ZnCl_2$ were added to the suspension. The resultant, enhanced fluorescence intensity,

dx.doi.org/10.1021/ic200478q |*Inorg. Chem.* 2011, 50, 7563–7573

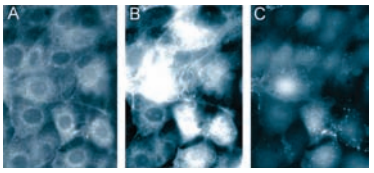

Figure 2. Fluorescence micrograph images of cellular Zn^{2+} observed after exposure to the Zn^{2+} fluorophore TSQ. (A) LLC-PK_1 cells incubated with 30 μM TSQ in DPBS for 30 min at 37 °C. (B) Fluorescence increase of A after addition of 30 μM Zn^{2+} and 3 μM pyrithione for 1 min. (C) Fluorescence reduction of B following addition of 100 μM TPEN for 10 min.

recorded as F_{max}, was converted to a concentration of $Zn(TSQ)_2$ and then to a concentration of TSQ using a linear standard curve of fluorescence emission intensity with increasing TSQ in DPBS containing 100 μM $ZnCl_2$. The initial intracellular concentration of TSQ reactive Zn^{2+} was then calculated by plotting the original fluorescence signal, F, on a calibration curve generated by titration of $ZnCl_2$ into DPBS containing a constant amount of TSQ equivalent to the total cellular TSQ previously determined. All data were normalized to the number of cells in the cuvette; reported values are an average of six measurements obtained in two triplicate experiments.

Sephadex G-75 Chromatography. Cells were grown in batches of 100-mm culture plates with media changes every 48 h. After cells reached confluence, the medium was decanted from the plates and cells were rinsed three times with cold DPBS. Cells were released from plates using 10× trypsin solution without EDTA (Sigma), pooled in cold DPBS, and collected by centrifugation. The pellet was resuspended with cold water and the cell membrane was disrupted by sonication. The homogenate was centrifuged for 35 min at 100 000g. The resultant supernatant was referred to as cytosol and loaded onto an 85 cm ×0.75 cm Sephadex G-75 gel filtration column, prepared as follows: Sephadex G-75 beads (GE Healthcare) were hydrated in 20 mM Tris-Cl, pH 7.4, and degassed by aspiration for approximately 30 min prior to pouring the chromatography column. The columns were equilibrated with degassed 20 mM TrisCl, pH 7.4. After addition of the sample to the column, a gravity reservoir containing 1 L of degassed 20 mM Tris-Cl was then attached and 1-mL fractions were collected. The void volume was ~8 mL. Based on molecular weight standards, fractions 10−20 contained molecules larger than 10 kDa; fractions 20−30 included molecules 10 kDa in size, and fractions 30−40 contained the low molecular weight species.

Atomic Absorption Spectrophotometry and Cell Digestion. The metal content of solutions was measured by flame atomic absorption spectrophotometry (AAS). The GBC model 904AA instrument atomized samples with an acetylene torch using an 80:20 mix of compressed air and acetylene. Measurements were obtained with a Zn element lamp and a deuterium background lamp. Data acquisition was performed in running mean mode and calibrated prior to each run using standards of 7.7, 15.4, and 30.8 μM Zn^{2+} that correspond to 0.5, 1.0, and 2.0 μg/mL Zn^{2+}.

Some measurements were made on digested cells. Digestion was conducted in 10% HNO_3 (ultrapure grade) for 1 h at 70 °C. After centrifugation, the supernatant was analyzed for Zn^{2+} content.

TSQ Fluorescence of G-75 Fractions. Fractions from the Sephadex G-75 chromatography separation were analyzed for TSQ fluorescence using a Hitachi F4500 spectrofluorometer. Fractions (1 mL) from TSQ stained cells and cytosol were placed directly in the cuvette and their emission intensity or fluorescence spectra were recorded. Corresponding fractions from unstained cells and cytosol were analyzed for their fluorescence properties after adding 10 μL of 1 mM TSQ and allowing 30 min to react.

Kinetics of Reaction of Apo-Metallothionein with Zn-$(TSQ)_2$. The loss of fluorescent intensity during the reaction of apo-metallothionein (apo-MT) with $Zn(TSQ)_2$ was plotted as a first order process. Two steps were revealed, with the slower one being pseudo-first order. When the extrapolated fluorescence emission from the second phase was subtracted from the overall intensity, both steps were revealed as pseudo-first-order reactions. The intensity of each phase at time zero revealed the fraction of reaction assigned to each reaction.

Preparation of Zn- and Apo-Carbonic Anhydrase and Other Zn-Proteins. Bovine serum carbonic anhydrase (CA) was purchased from Sigma. Protein (20 mg/mL) was prepared by dissolving the lyophilized sample in degassed 50 mM Tris-SO_4 buffer, containing 0.1 M $MgSO_4$, pH 8.0. Zn^{2+} deficient CA was prepared by a standard method in which Zn^{2+} was slowly removed from the protein by the competing chelating agent, 2,6-diaminopyridine.[29]

Bovine erythrocyte alkaline phosphatase (AP) was purchased from Sigma. The protein was prepared to a concentration of 25 mg/mL by dissolving in degassed 50 mM HEPES and 0.1 M KNO_3 buffer, pH 7.2. Yeast alcohol dehydrogenase was purchased from Worthington Biochemical Corporation. The protein was prepared by dissolving the lyophilized powder in degassed 20 mM Tris-Cl buffer, pH 7.4, to a final concentration of 10 mg/mL. Excess $ZnCl_2$ was added and the protein solution was chromatographed over a Sephadex G-15 column. Fractions were assayed for Zn^{2+} by AAS and protein by Lowry Assay (BIO-Rad DC Protein Kit).

A 25 amino acid zinc-finger peptide (sequence: KNFTCPECDLRFTTKANMKKHQRTHNI) based on the third finger of transcription factor TFIIIA from frog oocytes was synthesized using a peptide synthesizer and snap frozen with liquid nitrogen.[30] Prior to use in TSQ experiments the sample was thawed and mixed with excess $ZnCl_2$ and 2-mercaptoethanol. The mixture was then chromatographed on a Sephadex G-15 column equilibrated with 20 mM Tris-Cl, pH 7.4, to remove excess Zn^{2+} and the peptide fractions were identified by AAS.

Sephadex G-15 Isolation of TSQ-Zn-Carbonic Anhydrase. Carbonic anhydrase (50 nmol) was allowed to react with 50 nmol TSQ in a total of 250 μL of 50 mM Tris-SO_4 buffer for 15 min at room temperature. The reaction mixture was then loaded onto a 50 cm × 0.5 cm Sephadex G-15 column equilibrated with Tris-SO_4 buffer. Separation was performed at a constant flow of 1 mL/min using a peristaltic pump; 20 drop (1 mL) fractions were collected. Fractions were analyzed for TSQ fluorescence as described above and Zn^{2+} concentration by AAS. Void volume was typically 6 mL and the protein eluted in fractions 7−10.

Calculation of TSQ-Zn-Protein Dissociation Constants. Determination of the dissociation constant (K_d) was achieved after titrating TSQ into a set concentration of metalloprotein. The signal intensity at the wavelength of maximum emission was then converted to a value of fractional saturation, f:

$$f = (F - F_{min})/(F_{max} - F_{min}) \quad (4)$$

and

$$f = [TSQ]_{free}/([TSQ]_{free} + K_d) \quad (5)$$

where $[TSQ]_{free} = [TSQ]_{total} - [TSQ\text{-Zn-protein}]$. Curve fitting of experimental data to eq 5 was done using the SOLVER function of Microsoft Excel, which employs an iterative least-squares fitting method.

RESULTS

Toxicity of TSQ, Pryithione, and TPEN. LLC-PK_1 cells were treated with a range of TSQ concentrations for 1 and 24 h. Concentrations up to 300 μM TSQ did not compromise viability during 1 h incubations; 30 μM TSQ was innocuous over a 24 h span. PYR was nontoxic up to 3 μM during 30 min incubation.

dx.doi.org/10.1021/ic200478q |*Inorg. Chem.* 2011, 50, 7563–7573

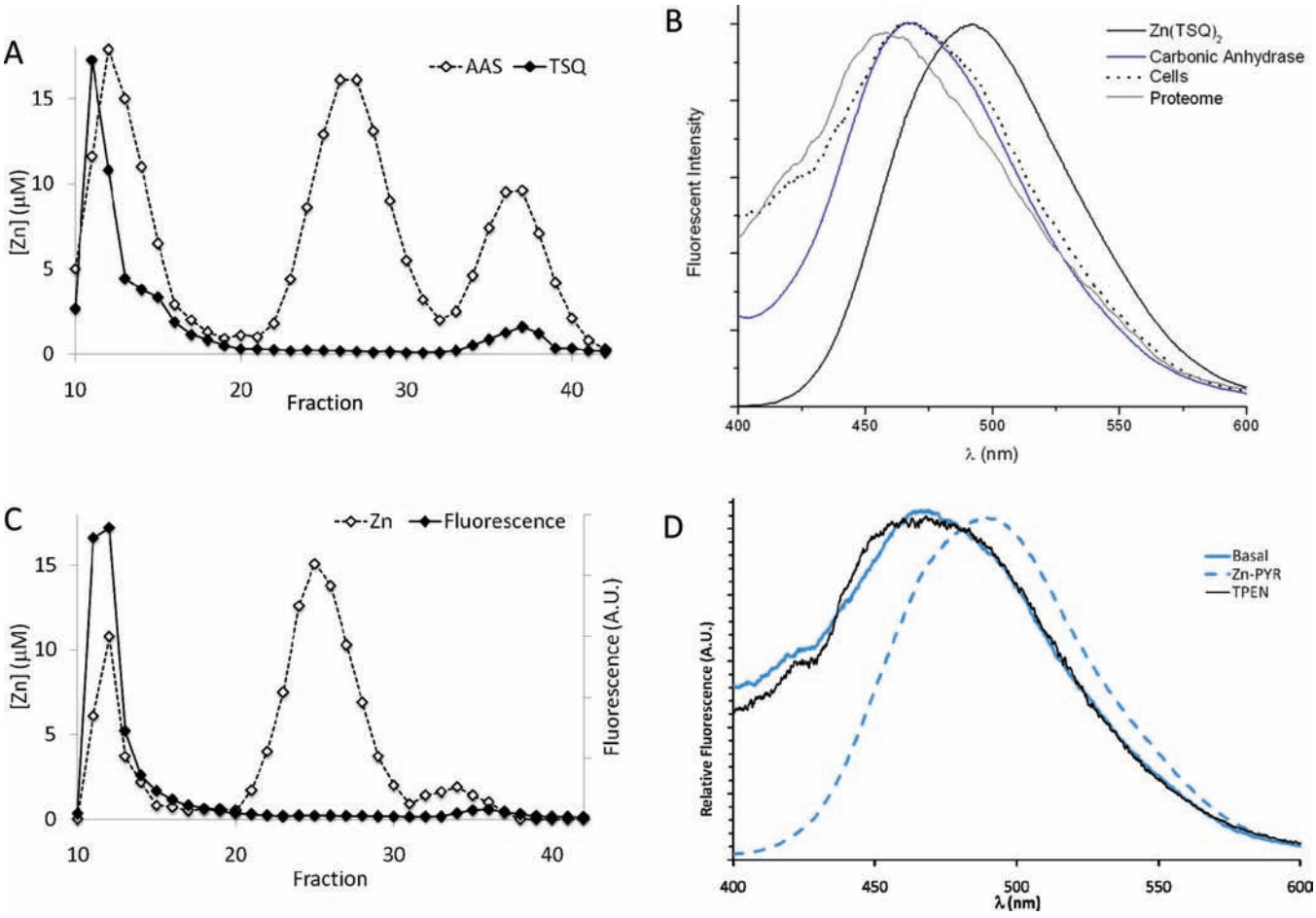

Figure 3. TSQ reaction with LLC-PK$_1$ cytosolic fractions and whole cells. (A) Sephadex G-75 chromatogram of the cytosolic fraction from 10^8 cells. Zn^{2+} in each fraction was quantified by AAS and by incubation with 10 μM TSQ for 30 min. (B) Fluorescence emission spectra of TSQ allowed to react with various Zn^{2+} sources: 5 μM $Zn(TSQ)_2$ (solid), 10 μM TSQ allowed to react with proteome from 10^8 cells (gray, Figure 3A), proteome isolated from TSQ stained cells (dotted, Figure 3C), and 10 μM TSQ allowed to react with 30 μM carbonic anhydrase (blue). (C) Gel filtration separation of supernatant from 10^8 cells stained with 30 μM TSQ for 30 min at 37 °C prior to isolation of cytosol. (D) Fluorescence emission spectra of whole cells allowed to react with TSQ. Cells stained 30 min with 30 μM TSQ (blue), then following addition of 30 μM $ZnCl_2$ and 3 μM pyrithione (dotted), and these cells treated with 100 μM TPEN (black). Spectral intensities were equalized to emphasize the shift in λ_{max}.

Lastly, 100 μM TPEN did not reduce cell viability following 1 h incubation.

TSQ Imaging of Cellular Zn^{2+}. As the foundation for this study, the fluorescent microscopic properties of TSQ were characterized under typical staining conditions using LLC-PK$_1$ cells. Figure 2A shows the typical fluorescence pattern of TSQ stained LLC-PK$_1$ cells. In the absence of Zn^{2+}, TSQ does not fluoresce.[21,22] Untreated cells did not fluoresce under the microscopic conditions used. Therefore, the microscopic emission pattern observed represents solely the interaction of the sensor with Zn^{2+}. The emission pattern was highlighted by intense punctate staining surrounding the nucleus, extending out into the cytoplasm, layered on a diffuse fluorescent background throughout the cell. Fluorescence was noticeably diminished in the nucleus.

The heavy metal chelators PYR and TPEN are commonly employed to demonstrate the Zn^{2+} dependence of the observed fluorescence. Excess Zn^{2+} is rapidly transported across the extracellular membrane following addition of 3 μM PYR and 30 μM $ZnCl_2$ to the extracellular medium. The resultant microscopic image in Figure 2B revealed a saturating enhancement in fluorescence emission within seconds that was distributed throughout many of the cells including their nuclei. This enhanced fluorescence was presumably due to the appearance of $Zn(TSQ)_2$ formed by the reaction of $Zn(PYR)_2$ with the excess free TSQ present in the cell according to reaction 6. The diffuse nature of the fluorescence was indicative of the formation of $Zn(TSQ)_2$ which, as an uncharged molecule with substantial nonpolar character, dispersed throughout the cytoplasm and organelles, including the nucleus. The exposure time was kept constant for all images in order to maintain qualitative comparability of fluorescence. Spectrofluorometric experiments presented below showed quantitatively that a 400% increase in fluorescence intensity followed $Zn(PYR)_2$ exposure. The increased fluorescence in the cells remained constant for at least 15 min.

$$Zn(PYR)_2 + 2TSQ \rightleftharpoons Zn(TSQ)_2 + 2PYR \qquad (6)$$

Finally, cells were allowed to react with 100 μM TPEN, a cell-permeant, high-affinity Zn^{2+} chelator commonly used to demonstrate a Zn^{2+} dependence of an observed fluorescence increase.

dx.doi.org/10.1021/ic200478q |*Inorg. Chem.* 2011, 50, 7563–7573

The observed decrease in fluorescence intensity was biphasic and incomplete, leaving some unquenched fluorescence in both the cytoplasm and the nucleus. An immediate and rapid loss of fluorescence was followed by a slower decay that continued for at least 10 min (Figure 2C). This incomplete quenching of basal TSQ-Zn^{2+} fluorescence was confirmed in another experiment by reacting TSQ stained cells with 100 μM TPEN for 30 min in the absence of an intermediate exposure to $Zn(PYR)_2$. The observed fluorescence gradually decreased to 30% of the initial signal within 10 min and remained constant for another 20 min. TPEN was added in sufficient excess to chelate all available Zn^{2+} in the sample according to reaction 7. Considering the large difference in Zn^{2+} affinity between TPEN ($\log K = 17.6\ M^{-1}$) and TSQ, no residual fluorescence was anticipated.[21,31]

$$Zn(TSQ)_2 + TPEN \rightleftharpoons Zn\text{-}TPEN + 2TSQ \quad (7)$$

Concentration of Cellular Zn^{2+} Imaged by TSQ. Microscopic data provided information on the intracellular and temporal distribution of Zn^{2+}-dependent fluorescence. However, variables such as cell thickness and intracellular fluorophore concentration prevented quantitative measurements of intracellular concentrations of fluorescent Zn-TSQ species by microscopy. Instead, these were acquired by using spectrofluorometry with cells suspended in a cuvette. The total intracellular concentration of TSQ in LLC-PK_1 cells was measured after saturating TSQ stained cells with Zn^{2+} supplied as 100 μM $Zn(PYR)_2$. The observed fluorescence was converted to a concentration of $Zn(TSQ)_2$ and then to TSQ concentration using a standard curve of increasing TSQ in PBS containing 100 μM $ZnCl_2$. It was found that 29 $\pm$ 8 nmol TSQ/10^6 cells accumulate within the cells during a 30 min exposure to 30 μM TSQ. Similarly, the concentration of Zn^{2+} bound to TSQ was measured as 0.71 $\pm$ 0.14 nmol $Zn^{2+}/10^6$ cells, based on the fluorescence intensity of TSQ stained cells prior to adding $Zn(PYR)_2$ and using a standard curve of $Zn(TSQ)_2$ fluorescence vs concentration of $Zn(TSQ)_2$. According to atomic absorption spectrophotometry of digested cells, the total Zn^{2+} content was 9.1 $\pm$ 1.8 nmol $Zn^{2+}/10^6$ cells. These results indicate that 8% of all cellular Zn^{2+} reacted with TSQ. This calculation assumed that a standard curve based on $Zn(TSQ)_2$ fluorescence could serve as a surrogate for the fluorescence properties of the unknown Zn-TSQ species. We also used a standard curve of TSQ-Zn-carbonic anhydrase (see below) instead of $Zn(TSQ)_2$. The quantum yield of TSQ-Zn-CA is less than that of $Zn(TSQ)_2$. As a result, the total concentration of Zn-protein imaged by TSQ increased to 2.2 $\pm$ 1.0 nmol/10^6 cells or 24% of all intracellular Zn^{2+}.

Fractionation of Supernatant Zn^{2+} Species. The observed microscopic and spectrofluorometric fluorescence of TSQ treated cells demonstrated that TSQ reacts with cellular Zn^{2+}. However, the sources of TSQ reactive Zn^{2+} have not been previously identified. To address this central issue, experiments with intact cells were complemented with studies on the reaction of TSQ with isolated cellular Zn^{2+} pools.

Cell supernatant was prepared from LLC-PK_1 cells that had been induced to synthesize Zn-MT by incubation with Zn^{2+}. Upon fractionation by gel filtration chromatography, three Zn^{2+} pools were separated, high molecular weight Zn-proteome (I) that includes the entire collection of cytosolic Zn-proteins greater than 10 kDa; metallothionein (II) which elutes as a 10 kDa species; and low molecular weight Zn^{2+} (LMW; III) (Figure 3A). The exact nature of the LMW Zn^{2+} pool has not been identified. By mass balance, these three pools accounted for all of the Zn^{2+} in the original sample.

Pool II was characterized in several ways. First, upon incubation of supernatant with Cd^{2+}, the band was converted to a Cd-protein that had the characteristic absorbance shoulder centered at 250 nm of Cd-MT as well as its proper ratio of SH:Cd^{2+} of 2.9.[32] The Cd-protein was further purified with DEAE ion-exchange chromatography. A single band was eluted at 2.8 mSieman, consistent with its identification as a metallothionein.[32] Amino acid analysis of the band revealed MT's characteristic high SH, basic amino acid, and serine content as well as its paucity of aromatic and other nonpolar amino acid residues (Supporting Information Table 1). Based upon analysis of its Zn^{2+} and SH content, as well as the Cd^{2+}:SH stoichiometry obtained after chromatography of supernatant exposed to a saturating concentration of Cd^{2+}, the native protein was only 76% saturated with Zn^{2+} and contained 2.1 nmol/10^7 cells of Zn^{2+} free sites.[33]

Analysis of TSQ Reactivity of Supernatant Fractions. TSQ was added to each isolated fraction, following the chromatographic separation of LLC-PK_1 cell supernatant, and the resultant fluorescence was measured. As seen in Figure 3A, almost all of the detectable fluorescence intensity was confined to the Zn-proteome. Little or no fluorescence was associated with the metallothionein or LMW fractions. Rechromatography of the fluorescent TSQ-Zn-proteome reaction mixture did not shift either fluorescence or Zn^{2+} into the LMW region. Fluorescence associated with TSQ that had been added directly to isolated supernatant prior to chromatography also localized in the Zn-proteome pool and did so without observable reorganization of Zn^{2+} among the separated pools. The same experiment conducted with supernatant from LLC-PK_1 cells that had not been induced with Zn^{2+} to synthesize measurable MT yielded identical results.

These results indicated that TSQ fluorescence in isolated supernatant was the result of TSQ reaction with a high molecular weight (>10 kDa) Zn^{2+} species. Furthermore, the products of this reaction remained bound within the proteome and chromatographed as high molecular weight species. In sum, these findings are consistent with the identification of the fluorescent products as TSQ-Zn-protein adducts as hypothesized in reaction 3.

Fluorescence Emission Spectra of Chromatographically Separated Supernatant Fractions Exposed to TSQ. Further evidence in support of the presence of TSQ-Zn-protein species in these cells was found in the fluorescence spectral analysis of the isolated fractions. Fluorescence emission spectra of TSQ treated protein fractions were markedly different from that of Zn-$(TSQ)_2$. The λ_{max} of $Zn(TSQ)_2$ is 490 nm (Figure 3B).[18,21,22] In contrast, the fluorescence spectra of the TSQ reactive protein fractions in Figure 3A were characterized by a blue-shifted λ_{max} of 470 nm (Figure 3B).

Alternative possibilities were investigated that might account for the shifted λ_{max}. The fluorescence emission spectrum of $Zn(TSQ)_2$ was measured in 50 mM Tris-Cl at pH of 6.2, 7.4 (λ_{max} = 490 nm), and 9.0. Also tested was $Zn(TSQ)_2$ dissolved in water (487 nm) and various other solvents including DMSO (504 nm), acetone (494 nm), ethanol (496 nm), and octanol (493 nm). Although the fluorescent intensity varied with solvent, the λ_{max} remained at or above 487 nm in these media. That a nanoprecipitate of the complex might account for the wavelength shift was discounted after showing that centrifugation for 30 min

Table 1. TSQ-Zn^{2+} Fluorescence Emission Maximum and apoMT Content in Mammalian Cell Lines

cell line/suspension	TSQ fluorescence λ_{max} (nm)	Zn_7-metallothionein (nmol/10^8 cells)	apo-metallothionein[a] (nmol/10^8 cells)
LLC-PK_1[b], pig kidney tubule	470	13	3.0
TE-671[b], human muscle medulobastoma	472	10	4.0
U-87 MG, human glioblastoma	471	11	2.0[c]
C6, rat glioma	474	0[d]	0[d]
CCRF-CEM, lymphocytic leukemia	471	0[d]	0[d]
A549, human lung adenocarcinoma	475	0[d]	0[d]
mouse whole brain, neuronal-astrocyte suspension (90−98% neurons)[e]	474	0[d]	0[d]
mouse whole brain, cortex (90−98% neurons)[e]	474	0[d]	0[d]

[a] Apo-metallothionein, MT with unsaturated binding sites, detected by subtracting metals bound to protein from total metal binding sites available as indicated by the thiol concentration and cadmium saturation analysis.[29] [b] Cells treated 24 h with 40:M Zn^{2+} to induce the synthesis of MT. [c] Basal concentration of apo-MT. [d] No measurable Zn-MT or apo-MT according to Sephadex G-75 chromatographic analysis for MT Zn^{2+} or SH. [e] Suspension culture.

at 100 000*g* or filtration through a 0.2-μm filter did not alter the intensity or spectral characteristics of the emission spectrum.

We also considered the formation of $Ca(TSQ)_2$ as an alternative to $Zn(TSQ)_2$.[18,22] The calcium complex exhibited an emission maximum at 482 nm with a weak fluorescence yield that was 5% of the intensity yielded from an equivalent concentration of $Zn(TSQ)_2$. In agreement with earlier results, TSQ binds Ca^{2+} weakly such that 100 fold excess of Ca^{2+} did not react with 10 μM $Zn(TSQ)_2$.

With these emission spectral results in hand, LLC-PK_1 cells were incubated with TSQ as in the microscopy experiments. Supernatant was prepared and chromatographed by Sephadex G-75, and the fractions were assayed for TSQ fluorescence (Figure 3C). Again, the TSQ fluorescence primarily remained associated with the proteome. Furthermore, analysis of the emission spectra revealed a λ_{max} of 470 nm for the isolated proteome fractions (Figure 3B). Thus, the fluorescing supernatant fractions from TSQ-incubated cells closely resembled the spectrum of cell supernatant treated with TSQ.

Spectrofluorometry of TSQ-Treated Cells. Having gathered support from in vitro experiments for the presence of high molecular weight TSQ-Zn^{2+} ternary complexes, the procedure that led to the results shown in Figure 2 was repeated with the modification that TSQ stained cells were suspended in phosphate-buffered saline allowing for spectrofluorometric instead of microscopic analysis. The initial λ_{max} of TSQ stained cells was 470 nm as seen in Figure 3D. The blue-shifted spectrum indicated that $Zn(TSQ)_2$ was not present as the predominant species and implied the presence of TSQ-Zn^{2+} ternary complexes as observed in cell supernatant fractions.

When these cells were subsequently exposed to Zn^{2+} and PYR, as in Figure 2B, the TSQ fluorescence peak not only increased 4-fold but its emission spectrum also shifted to 490 nm, indicating the formation of $Zn(TSQ)_2$ as the primary fluorescent species (Figure 3D, all spectra normalized to the same maximum intensity). These data were consistent with the formation of $Zn(TSQ)_2$ after $Zn(PYR)_2$ rapidly distributed across the cell membrane and allowed to react by ligand substitution with free TSQ that was also distributed throughout the cells (reaction 6).

Addition of TPEN resulted in a biphasic loss of fluorescence. The 490 nm fluorescent emission was rapidly quenched in the first phase leaving a residual band centered at 470 nm with 30% of the initial fluorescence intensity, consistent with the microscopic results of Figure 2C (Figure 3D). The loss of all of the 490 nm centered fluorescence was consistent with the ligand substitution of TPEN with cellular $Zn(TSQ)_2$ according to the highly favorable equilibrium and kinetics of reaction 7. Reduction of the original 470 nm fluorescence occurred at the slower rate. This was interpreted as the result of the reaction of TPEN with TSQ-Zn^{2+} ternary complexes.

In another version of the experiment, cells were allowed to react with TPEN first and then with TSQ. As above, cells fluoresced with an emission spectrum that exhibited a λ_{max} of 470 nm and also displayed reduced fluorescence intensity consistent with the initial reaction of TPEN with some of the Zn^{2+} ligand complexes that otherwise react with TSQ. Previous experiments have documented that TPEN undergoes ligand substitution with approximately 30% of the Zn^{2+} bound in the Zn-proteome.[34] That result in concert with experiments reported here support the formation of TSQ-Zn-protein complexes that in large part are reactive with TPEN as in reaction 8.

$$\text{TPEN} + \text{TSQ-Zn-ligand} \rightleftharpoons \text{Zn-TPEN} + \text{ligand} + \text{TSQ} \quad (8)$$

Behavior of TSQ in Other Cell Types. The generality of the reaction of TSQ with cells was tested by repeating some of the experiments described above in an assortment of cultured cells. These included human muscle meduloblastoma (TE671) and glioblastoma (U-87 MG) cells, fetal mouse neurons and astrocytes (9:1 ratio), and other diverse cell lines (Table 1). In every case, cells exposed to TSQ displayed a fluorescence emission spectrum centered near 470 nm. Similarly, as with LLC-PK_1 cells, fluorescence was associated almost exclusively with the proteome fraction according to Sephadex G-75 chromatography of the supernatant from each of these cells and tissues (Supporting Information). Based on this survey, it was apparent that TSQ reacts similarly with a variety of different cell types, normal and transformed, from several species.

TSQ Reactions with Metallothionein. TSQ did not react with the metallothionein pool in LLC-PK_1 cells despite the relatively large concentration of Zn^{2+} bound to MT (Figure 3A). We probed this lack of reactivity using purified rabbit liver Zn_7-MT 2.[35] Addition of 0.14 μM Zn_7-MT (1 μM total Zn^{2+}) to 21.5 μM TSQ failed to increase fluorescence over 90 min. Adjusting the concentration to a 200-fold excess of TSQ relative to Zn^{2+} was also ineffective in stimulating fluorescence

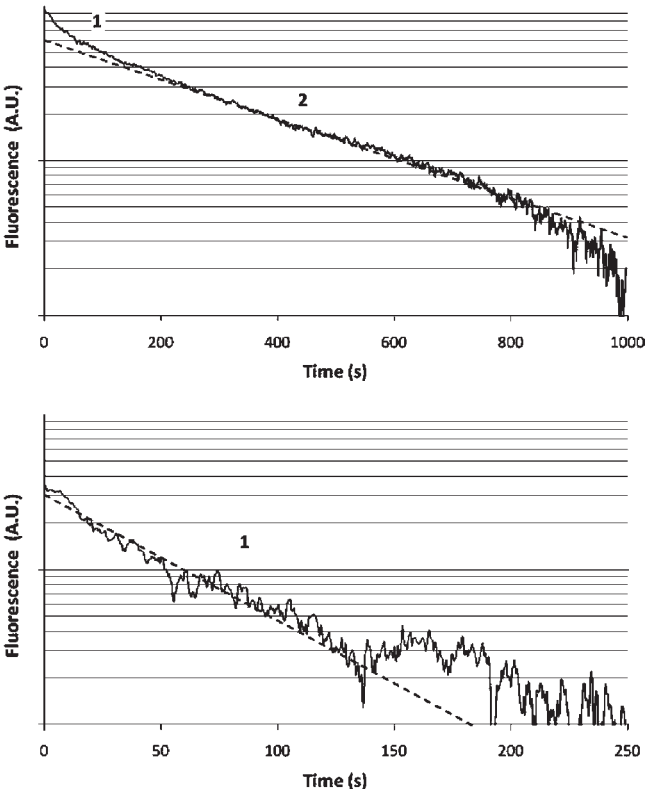

Figure 4. Reaction of TSQ with apo-metallothionein. Loss in fluorescence was monitored during the reaction of 1 μM apoMT with 1 μM $Zn(TSQ)_2$ at 25 °C in 50 mM Tris-Cl pH 7.4. The figure shows the loss of $Zn(TSQ)_2$ fluorescence plotted as two pseudo-first-order processes 1 and 2.

after 2 h of reaction. MT binds Zn^{2+} with an average stability constant of 2×10^{11} M.[33] TSQ was neither able to compete with MT protein for Zn^{2+} nor able to form a fluorescent adduct with Zn_7-MT.

The MT pool of LLC-PK_1 and U-87 cells (Table 1) contains metal free binding sites. At 3−4 nmol/10^8 cells, this represents 21−28 nmol Zn^{2+} binding sites/10^8 cells, the same order of magnitude but smaller than the estimated 70−220 nmol TSQ bound $Zn^{2+}/10^8$ cells. Thus, we also investigated the reactivity of apo-MT with $Zn(TSQ)_2$. Addition of 1 μM apo-MT (20 μM total thiol) to 1 μM $Zn(TSQ)_2$ resulted in a rapid loss of $Zn(TSQ)_2$ fluorescence with the intensity being reduced to 10% of its initial value within 10 min. When plotted as a first-order process, it was clear that the reaction was biphasic and characterized by two pseudo-first-order steps with rate constants of 1.47×10^{-2} s^{-1} and 9.34×10^{-2} s^{-1} (Figure 4). The fractions of reaction in the fast and slow phases were 0.37 and 0.63, respectively. The biphasic kinetics were consistent with the independent formation of the two metal clusters Zn_3S_9 and Zn_4S_{11}, which would comprise 0.43 and 0.57 of the total reaction. According to both equilibrium and kinetic analysis, the reaction of apo-MT with $Zn(TSQ)_2$ is favorable. Consequently, intracellular $Zn(TSQ)_2$ should readily react with apo-MT, thereby suppressing at least some of the fluorescence from $Zn(TSQ)_2$ in LLC-PK_1 and U-87 cells, assuming that the concentration of apo-MT is sufficiently large.

Model Reactions of TSQ with Zn-Proteins. Several Zn-proteins were utilized as models for assessing the properties of ternary, TSQ-Zn-protein formation. In an initial study, we considered the interaction of TSQ with Zn-carbonic anhydrase (Zn-CA). With a tightly bound Zn^{2+} ($K_D = 10^{-12}$ M) coordinated by three histidines at the base of a broad solvent accessible active site, Zn-CA seemed a likely reaction site for TSQ.[36,37] Indeed, the Zn^{2+} adduct formation reaction of Zn-CA, newly formed in vivo from apo-CA and Zn^{2+}, with dansylamide serves as the basis for another Zn^{2+} sensor method.[38] Figure 5A shows the result of a titration of Zn-CA with TSQ. The progressive reaction generated an increasingly intense emission spectrum with a spectral maximum at 470 nm, the same observed in cells incubated with TSQ and in chromatographed cytosolic proteome fractions. A similar titration of Zn-CA after chelation of most of its Zn^{2+} (0.2 Zn^{2+} per mol CA) displayed proportionately reduced fluorescence emission (data not shown).

The titration data above were used to calculate a K_d of $1.55 \pm 0.65 \times 10^{-7}$ M for the reaction of TSQ with Zn-CA (Figure 5B).

$$\text{TSQ} + \text{Zn-CA} \rightleftharpoons \text{TSQ-Zn-CA} \quad (9)$$

Gel filtration chromatography of the product demonstrated that TSQ and Zn^{2+} remained bound to the protein even after gel filtration, thereby confirming that a ternary adduct had been formed (Figure 5C). These results demonstrated that TSQ-based fluorescence resulted from ternary complex formation and was dependent on the presence of Zn^{2+} in the protein.

A similar titration of alcohol dehydrogenase resulted in an adduct characterized by a fluorescence emission spectrum with λ_{max} at 470 nm and TSQ dissociation constant of 4.86×10^{-5} M (Figure 5D). Spectra of the reaction of TSQ with alkaline phosphatase and a model zinc-finger peptide revealed emission maxima at 470 and 480 nm (Figure 5E). In each case, the blue-shifted fluorescence spectrum signaled the formation of a ternary TSQ-Zn-protein adduct. That a tetrahedrally coordinated Zn^{2+} site as in the Zn-finger peptide formed a ternary complex with TSQ is consistent with prior studies of the adduct forming capability of Zinquin with small Zn-complexes.[19]

DISCUSSION

Zinc biochemistry is remarkably rich. As many as 3000 Zn-proteins populate the mammalian proteome.[1,2] Besides its broad catalytic roles within the Zn-proteome, Zn^{2+} also serves as a structural determinant in many proteins, including various classes of zinc-finger transcription factors.[1] It is assumed that most of these proteins comprise a Zn-proteome that is common to the various cell types found in mammalian organisms. Other Zn-proteins are restricted to special cell types, such as Zn-proinsulin in pancreatic islet cells.[39]

TSQ and its analogue Zinquin have been employed routinely for nearly 20 years as biological Zn^{2+} sensors. They have been used in many different cell types and tissues to detect basal cellular Zn^{2+} and physiological and pathological changes in chelatable Zn^{2+}.[9,13,21,22,26,39−44] In the present study, we used LLC-PK_1, kidney proximal tubular cells as a typical cell and primary model system. Results in this cell line were then compared with findings in seven other diverse cell types (Table 1).

Our interest in kidney Zn^{2+} biochemistry relates to the mechanism of toxicity of Cd^{2+} in proximal tubular cells and the likelihood that it results from Cd^{2+} displacement of Zn^{2+} from key metalloproteins.[45] This type of metal ion exchange reaction is also thought to activate MTF-1, a metallothionein gene promoter transcription factor, by making labile Zn^{2+} available to bind to

dx.doi.org/10.1021/ic200478q |*Inorg. Chem.* 2011, 50, 7563–7573

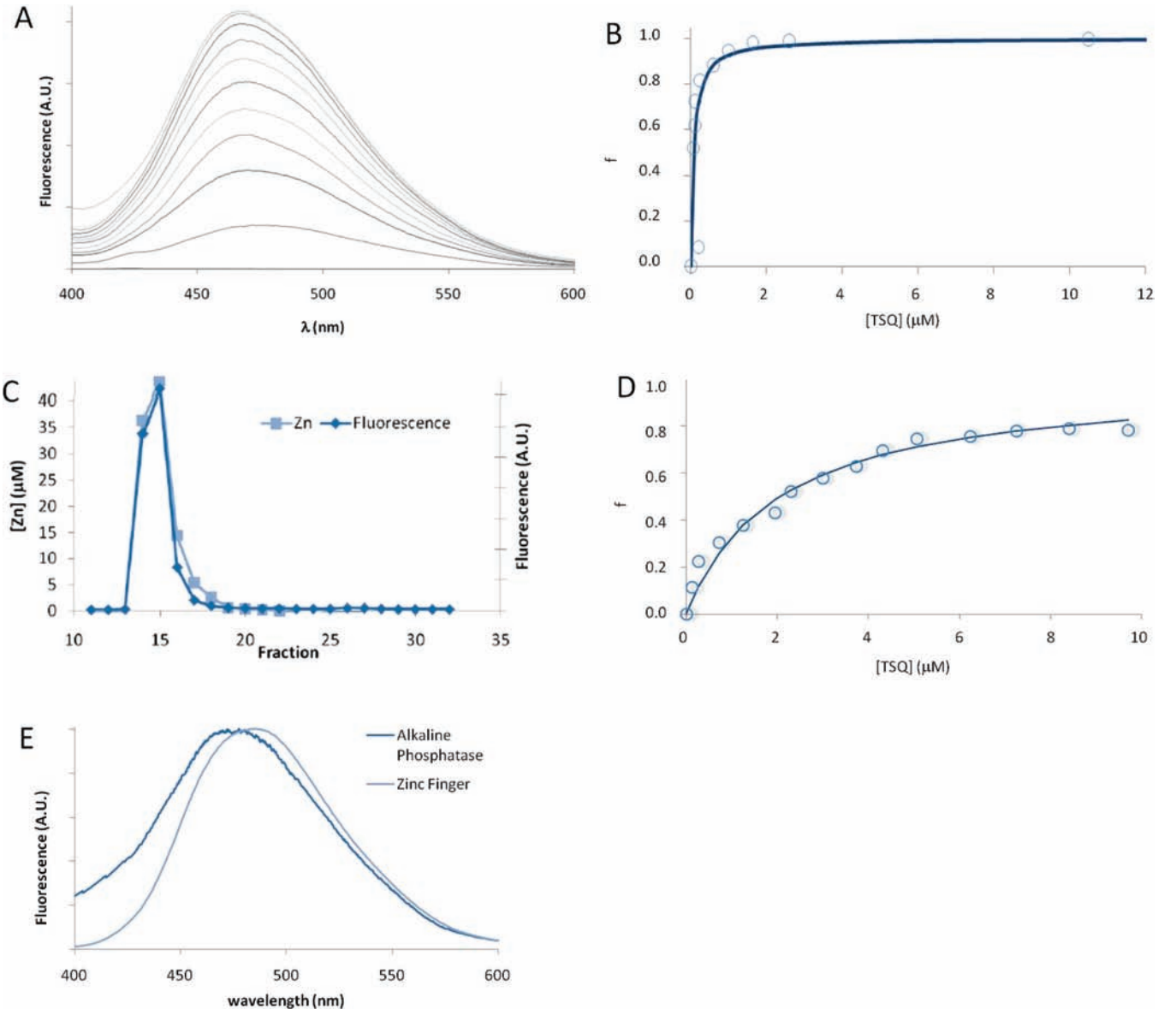

Figure 5. TSQ ternary binding with zinc proteins. (A) Fluorescent emission spectra of 10 μM carbonic anhydrase and increasing concentrations of TSQ in 50 mM Tris-SO_4, pH 7.4 at 25 °C. (B) Fractional saturation (f) vs concentration of free TSQ for the titration in A. Curve represents best fit to eq 5. (C) Sephadex G-15 size-exclusion chromatogram of a mixture of 50 nmol carbonic anhydrase and 50 nmol TSQ allowed to react for 15 min at 25 °C in 250 μL of 50 mM Tris-SO_4, pH 7.4. (D) Titration of 10 μM alcohol dehydrogenase with TSQ in 20 mM Tris-Cl pH 7.4 at 25 °C: Fractional saturation (f) vs concentration of free TSQ. Curve represents best fit to eq 5. (E) Fluorescence emission spectra of 10 μM TSQ allowed to react with 10 mg/mL alkaline phosphatase in 50 mM HEPES, pH 7.2 at 25 °C (dark blue); and 3 μM Zn^{2+}-finger peptide mF3 allowed to react with 5 μM TSQ in 20 mM Tris-Cl, pH 7.4 at 25 °C (light blue).

MTF-1 apo-zinc-finger motifs.[46,47]

$$\text{MTF-1} + Zn^{2+} \rightleftharpoons \text{Zn-MTF-1} \quad (10)$$

In turn, active MTF-1 stimulates MT synthesis that binds Cd^{2+} and protects the cell from its cytotoxic reactions.[46,48] Thus, basal Zn^{2+} distribution as well as Cd^{2+} induced changes in Zn^{2+} trafficking are potentially amenable to study with fluorescent Zn^{2+} sensors.

TSQ is a convenient Zn^{2+} fluorophore because it does not fluoresce in the absence of Zn^{2+} or in the presence of other physiological metal ions. Thus, in Figure 2, the observed fluorescence directly represents TSQ interacting with intracellular species of Zn^{2+}. The distribution of fluorescence within cells treated with TSQ resembles, qualitatively, micrographs presented in other studies (Figure 2A).[5,8,13,21] The distribution is asymmetric, largely concentrated outside and around the nucleus, and is to some extent punctate. Delivery of extra Zn^{2+} into the cells via the ionophoric complex, $Zn(PYR)_2$ greatly increased the fluorescence due to $Zn(TSQ)_2$, overexposing the picture (Figure 2B). Interestingly, newly formed $Zn(TSQ)_2$ was relatively uniformly distributed throughout the cell in contrast to the original fluorescent species. Lastly, TPEN, a high-affinity, cell-permeable ligand for Zn^{2+} and other metal ions, reversed the fluorescence increase caused by $Zn(PYR)_2$ and further diminished the original fluorescence in a two-step kinetic process (Figure 2C). The results with TPEN were

dx.doi.org/10.1021/ic200478q |*Inorg. Chem.* 2011, 50, 7563–7573

similar to those seen in other studies and supported the involvement of Zn^{2+} in the observed fluorescent species.[13,21]

The cellular distribution of $Zn(TSQ)_2$, produced by the intracellular reaction of $Zn(PYR)_2$ and TSQ, was symmetric and diffuse throughout the cell (Figure 2B). According to Figure 2C, TPEN had access to the $Zn(TSQ)_2$ as well as much of the basal TSQ-Zn^{2+} species. $Zn(PYR)_2$, TSQ, and $Zn(TSQ)_2$ are neutral complexes and TPEN migrates through membranes as a neutral structure. Thus, the results suggest that both TSQ and TPEN broadly access intracellular spaces and compartments. Alternatively, the wide distribution of $Zn(TSQ)_2$ might have resulted from its ability for facile movement throughout the cell. The observation that the original distribution of TSQ fluorescence was asymmetric implies that the Zn^{2+} species to which TSQ binds are, themselves, asymmetrically organized in the cell.

The inability to use TSQ as a quantitative Zn^{2+} fluorophore in microscopic experiments was overcome by examining the fluorescence properties of TSQ stained cells in suspension using a conventional spectrofluorometer. With this technique, fluorescence excitation and emission spectra were obtained under standard conditions of cell number and optical path length and used both to quantify the fluorescence by reference to a standard curve and to characterize the fluorescent properties of the Zn-TSQ species. The spectrofluorometric measurements demonstrated that TSQ was imaging a significant fraction of cellular Zn^{2+}, about 8% based on a standard curve of $Zn(TSQ)_2$ fluorescence. It has been shown that the total concentration of Zn^{2+} in cells is on the order of 10^{-4} to 10^{-3} M.[49] Therefore, TSQ images μM concentrations of Zn^{2+} not the nM or pM concentrations of chelatable Zn^{2+} as detected with sensors such as Fluozin-3.[49,50] Thus, either TSQ readily competed for significant concentrations of proteomic Zn^{2+} (reaction 11)

$$\text{Zn-protein} + 2\ \text{TSQ} \rightleftharpoons \text{Zn(TSQ)}_2 + \text{apo-protein} \quad (11)$$

or in some other way interacted with a substantial part of the cell's Zn^{2+} complement.

LLC-PK_1 cell volume has been calculated as about 4 pL/cell.[51] Thus, after incubation with TSQ, intracellular TSQ concentration was 7.2 mM (29 nmol/10^6 cells $\times$ 1 cell/4 $\times$ 10^{-12} L), more than 200 hundred times that of the outside medium and much larger than TSQ's aqueous solubility limit of about 12 μM at pH 7. From this calculation, it is inferred that much of the cellular TSQ is localized in membrane lipids.

Repeating the experiments summarized in Figure 2 with cell suspensions, it was observed that TSQ stained cells displayed a fluorescence emission spectrum with a wavelength maximum at 470 nm. In contrast, the spectrum of cells subsequently exposed to $Zn(PYR)_2$ shifted to 490 nm, the λ_{max} of free $Zn(TSQ)_2$. When TPEN quenched the fluorescence of these cells, all of the 490 nm fluorescence and 70% of the 470 nm fluorescence disappeared. The rapid loss of $Zn(TSQ)_2$ was anticipated because of the much larger stability constant of Zn-TPEN.[21] The fact that it did occur in the complex environment of the cell supported the capacity of TPEN, like $Zn(TSQ)_2$, to distribute itself uniformly throughout the cell.

Clearly, at least two different species were detected in this experiment: $Zn(TSQ)_2$ with its fluorescence emission spectrum centered at 490 nm and a TSQ-Zn^{2+} complex with a blue-shifted spectrum. Perhaps, the latter was $Zn(TSQ)_2$ in an environment that caused its emission spectrum to shift from 490 to 470 nm. Examination of $Zn(TSQ)_2$ in a variety of solvents, under conditions of acidity, and in different physical states did not reveal such a species. Fluorescence intensity changed with solvent but none of them shifted the emission maximum into the 470 nm range.[40] Moreover, the fact that TPEN did not completely quench the fluorescence of this species despite its large stability constant for Zn^{2+} and widespread cellular distribution also suggested that the Zn-TSQ species observed in the absence of added Zn^{2+} was not $Zn(TSQ)_2$.[31]

It has been shown that LLC-PK_1 cells incubated with Zn^{2+} and U-87 MG cells grown in standard medium contain 3−4 nmol/10^8 cells of apoMT (Table 1). This metal-unsaturated form of the protein has a large affinity for Zn^{2+} and reacts efficiently with $Zn(TSQ)_2$ in vitro.[35] Thus, its presence in cells opens up the possibility for ligand substitution (reaction 12).

$$\text{apo-MT} + \text{Zn(TSQ)}_2 \rightleftharpoons \text{Zn-MT} + 2\text{TSQ} \quad (12)$$

If the fluorescence were due to the formation of $Zn(TSQ)_2$, the presence of apo-MT would quench some of the total observed TSQ fluorescence, estimated at 70−200 nmol/10^8 cells, as Zn^{2+} was transferred from $Zn(TSQ)_2$ into the MT pool. However, the presence of TSQ did not shift Zn^{2+} into MT. This finding argued that the observed fluorescence was not a result of the formation of $Zn(TSQ)_2$.

An earlier in vivo study with TSQ concluded that TSQ does react with Zn^{2+} bound to MT.[52] According to the in vitro results above (reaction 12), it is the reverse reaction that is favorable even in the presence of a large excess of TSQ. A recent paper by Maret and Krezel proposed that one of MT's complement of seven Zn^{2+} ions has a low binding constant.[53] Conceivably, that site might be reactive with TSQ. However, in subsequent experiments, we demonstrated that MT prepared at pH 7 uniformly binds Zn^{2+} with average stability constants of $10^{11.2}$ M.[35] Native MT can be converted to the Maret−Krezel protein by brief exposure to acid conditions at pH 2. Another report suggested that Zinquin undergoes ligand substitution with Zn-MT.[54] Because Zinquin binds Zn^{2+} with higher affinity than TSQ, that reaction might be favorable.

To begin to understand the molecular nature of the cellular Zn-TSQ species, cells preincubated with TSQ were sonicated and the resulting supernatant fractionated by gel filtration. According to Figure 3C, virtually all of the TSQ fluorescence was located in the Zn-proteome band, despite the presence of other large Zn^{2+} pools in the MT and LMW fractions. In agreement with the cellular results, the fluorescence emission spectra of the isolated proteomic fractions were characterized by wavelength maxima of 470 nm. Similar results were obtained when cell supernatant was first isolated and then either allowed to react with TSQ before gel filtration or after it was fractionated. As in cells, the addition of TPEN to the mixture of TSQ and Zn-proteome resulted in a slow, incomplete decline in fluorescence. Therefore, a self-consistent picture emerged from cellular and supernatant studies: TSQ allowed to react with Zn^{2+} in the Zn-proteome formed species characterized by a spectral λ_{max} that was blue-shifted from that of $Zn(TSQ)_2$. Spectroscopy and chromatographic data give no evidence of $Zn(TSQ)_2$ formation in cell supernatant and instead supported the formation of ternary adducts as hypothesized in reaction 3.

This hypothesis also found strong support in an earlier study of the reaction of the TSQ analog, Zinquin (Zinquin, ethyl[2-methyl-8-*p*-toluenesulfonamido-6-quinolyloxy]acetate), ZQ) with

dx.doi.org/10.1021/ic200478q |*Inorg. Chem.* 2011, 50, 7563–7573

a number of small molecular Zn^{2+} complexes.[19] It was shown with a number of Zn^{2+} ligand frameworks in which Zn^{2+} was either 3- or 4-coordinate, that the adducts formed with ZQ invariably displayed blue-shifted emission spectra relative to $Zn(ZQ)_2$.

The experiments described above for LLC-PK_1 were repeated with a diversity of other cell types. As shown in Table 1, each cell or tissue type displayed closely similar fluorescent properties when exposed to TSQ. Thus, according to this initial survey, it appears that there is some generality to the behavior of TSQ as it interacts with cellular Zn^{2+} pools. In turn, the results also suggest that the Zn-proteomic sites that are available to react with TSQ share common properties across a diversity of cells.

In order to test our hypothesis of TSQ-Zn-protein adduct formation, several Zn^{2+} binding proteins were chosen for model studies. As a starting point, the reaction of TSQ with Zn-CA was analyzed. TSQ allowed to react with Zn-CA to form a 1:1 adduct characterized by a spectral λ_{max} of 470 nm and a dissociation constant of 1.55×10^{-7} M. The reaction did not occur in the absence of CA bound Zn^{2+} or in the presence of the Zn-CA inhibitor, dansylamide that displaces TSQ from the protein. The results are consistent with the reaction

$$\text{TSQ} + \text{Zn-CA} \rightleftharpoons \text{TSQ-Zn-CA} \qquad (13)$$

Several other Zn^{2+} proteins also formed ternary TSQ-Zn-protein complexes, based upon the appearance of blue-shifted TSQ-Zn fluorescence spectra and association of the fluorophore with the proteins as judged by Sephadex chromatography. Together with the cellular data, these results solidified the conclusion that TSQ-Zn-protein complexes form in vivo.

This redefinition of the nature of the molecular species that fluoresce in cells exposed to TSQ implies that the observed microscopic fluorescence distribution represents the spatial distribution of a subset of Zn-proteins in the Zn-proteome. What that means in terms of cell structure and function remains to be determined. The next step to assess the significance of this relationship will be to determine which members of the Zn-proteome participate in TSQ-Zn-protein adducts. Preliminary chromatographic and electrophoretic separations have isolated fractions that selectively react with TSQ but much remains to be done to obtain and identify pure ternary complexes.

In recent years, the TSQ analog ZQ has been touted as an improved sensor because its ester form can be hydrolyzed by cellular hydrolases, leaving the membrane-impermeable acid form trapped inside the cell.[21] In studies to be published elsewhere, we have found that ZQ also forms ZQ-Zn-protein adducts that display blue-shifted fluorescence emission spectra in comparison with $Zn(ZQ)_2$.

CONCLUSIONS

The results of this study suggest that when previous studies detected basal Zn^{2+} with TSQ, they were imaging substantial concentrations of proteomic Zn^{2+} and not miniscule amounts of Zn^{2+} in the nM or pM range. The fundamental redefinition of what these sensors are capable of imaging necessitates a reexamination of whether past studies that utilized TSQ or ZQ also imaged TSQ-Zn-protein and ZQ-Zn-protein complexes. Moreover, the possibility now exists that observed cellular fluorescence can be connected with the actual intracellular Zn^{2+} binding sites. This new understanding presents an opportunity to explore Zn^{2+} trafficking and its functions in relation to the participation and spatial distribution of the Zn^{2+} proteins responsible for the observed fluorescence.

ASSOCIATED CONTENT

Supporting Information. Figures S1 and S2, Table S1. This material is available free of charge via the Internet at http://pubs.acs.org.

AUTHOR INFORMATION

Corresponding Author

*Phone: 1 414 229 5853; fax: 1 414 229 5530; e-mail: petering@uwm.edu.

Present Addresses

[§]Department of Laboratory Medicine and Pathology, Mayo Clinic, Rochester, MN 55905.

ACKNOWLEDGMENT

Funding was made possible by the NIH grants GM-85114, ES-04026, and ES-04184. Initial funds were from the University of Wisconsin—Milwaukee Research Growth Initiative. Microscopy was conducted in the Children's Environmental Health Sciences Core Center Imaging and Histology Laboratory. We thank the laboratory of Dr. Douglas Lobner for the samples of neonatal brain cell suspensions, Dr. Christopher Chitambar at the Medical College of Wisconsin who provided the CCRF-CEM cell line, Dr. Sara Krull in the laboratory of Dr. Petering for the MT amino acid analytical data, and Mohammad Namdarghanbari who contributed to the calculation of the dissociation constant of TSQ-Zn-CA.

REFERENCES

(1) Andreini, C.; Banci, L.; Bertini, I.; Rosato, A. *J. Proteome Res.* **2006**, *5*, 196–201.
(2) Andreini, C.; Banci, L.; Bertini, I.; Rosato, A. *J. Proteome Res.* **2006**, *5*, 3173–8.
(3) Paoletti, P.; Vergnano, A. M.; Barbour, B.; Casado, M. *Neuroscience* **2009**, *158*, 126–36.
(4) Li, H.; Cao, R.; Wasserloos, K. J.; Bernal, P.; Liu, Z. Q.; Pitt, B. R.; St. Croix, C. M. *Ann. N.Y. Acad. Sci.* **2010**, *1203*, 73–8.
(5) Lim, N. C.; Freake, H. C.; Bruckner, C. *Chem.—Eur. J.* **2004**, *11*, 38–49.
(6) Tomat, E.; Lippard, S. J. *Curr. Opin. Chem. Biol.* **2010**, *14*, 225–30.
(7) Domaille, D. W.; Que, E. L.; Chang, C. J. *Nat. Chem. Biol.* **2008**, *4*, 168–75.
(8) Budde, T.; Minta, A.; White, J. A.; Kay, A. R. *Neuroscience* **1997**, *79*, 347–58.
(9) Lu, Y. M.; Taverna, F. A.; Tu, R.; Ackerley, C. A.; Wang, Y. T.; Roder, J. *Synapse* **2000**, *38*, 187–97.
(10) Koh, J. Y.; Suh, S. W.; Gwag, B. J.; He, Y. Y.; Hsu, C. Y.; Choi, D. W. *Science* **1996**, *272*, 1013–1016.
(11) Tonder, N.; Johansen, F. F.; Frederickson, C. J.; Zimmer, J.; Diemer, N. H. *Neurosci. Lett.* **1990**, *109*, 247–52.
(12) Tsuchiya, D.; Hong, S.; Suh, S. W.; Kayama, T.; Panter, S. S.; Weinstein, P. R. *J. Cereb. Blood Flow Metab.* **2002**, *22*, 1231–8.
(13) St Croix, C. M.; Wasserloos, K. J.; Dineley, K. E.; Reynolds, I. J.; Levitan, E. S.; Pitt, B. R. *Am. J. Physiol.* **2002**, *282*, L185–92.
(14) Tang, Z. L.; Wasserloos, K.; St. Croix, C. M.; Pitt, B. R. *Am. J. Physiol.* **2001**, *281*, L243–L249.
(15) Pearce, L. L.; Wasserloos, K.; St. Croix, C. M.; Gandley, R.; Levitan, E. S.; Pitt, B. R. *J. Nutr.* **2000**, *130*, 1467S–70S.

(16) Petering, D. H. *Chemtracts: Inorg. Chem.* **2004**, *17*, 569–580.
(17) Outten, C. E.; O'Halloran, T. V. *Science* **2001**, *292*, 2488–92.
(18) Frederickson, C. J.; Kasarskis, E. J.; Ringo, D.; Frederickson, R. E. *J. Neurosci. Methods* **1987**, *20*, 91–103.
(19) Hendrickson, K. M.; Geue, J. P.; Wyness, O.; Lincoln, S. F.; Ward, A. D. *J. Am. Chem. Soc.* **2003**, *125*, 3889–3895.
(20) Jindal, R. M.; Taylor, R. P.; Gray, D. W.; Esmeraldo, R.; Morris, P. J. *Diabetes* **1992**, *41*, 1056–62.
(21) Nasir, M. S.; Fahrni, C. J.; Suhy, D. A.; Kolodsick, K. J.; Singer, C. P.; O'Halloran, T. V. *J. Biol. Inorg. Chem.* **1999**, *4*, 775–83.
(22) Reyes, J. G.; Santander, M.; Martinez, P. L.; Arce, R.; Benos, D. J. *Biol. Res.* **1994**, *27*, 49–56.
(23) Suh, S. W.; Frederickson, C. J.; Danscher, G. *J. Cereb. Blood Flow Metab.* **2006**, *26*, 161–9.
(24) Varea, E.; Ponsoda, X.; Molowny, A.; Danscher, G.; Lopez-Garcia, C. *J. Neurosci. Methods* **2001**, *110*, 57–63.
(25) Zalewski, P.; Truong-Tran, A.; Lincoln, S.; Ward, D.; Shankar, A.; Coyle, P.; Jayaram, L.; Copley, A.; Grosser, D.; Murgia, C.; Lang, C.; Ruffin, R. *BioTechniques* **2006**, *40*, 509–520.
(26) Zalewski, P. D.; Forbes, I. J.; Betts, W. H. *Biochem. J.* **1993**, *296*, 403–8.
(27) Fahrni, C. J.; O'Halloran, T. V. *J. Am. Chem. Soc.* **1999**, *121*, 11448–11458.
(28) Hatok, J.; Babusikova, E.; Matakova, T.; Mistuna, D.; Dobrota, D.; Racay, P. *Clin. Exp. Med.* **2009**, *9*, 1–7.
(29) Hunt, J. B.; Rhee, M. J.; Storm, C. B. *Anal. Biochem.* **1977**, *79*, 614–7.
(30) Krepkiy, D.; Forsterling, F. H.; Petering, D. H. *Chem. Res. Toxicol.* **2004**, *17*, 863–870.
(31) Anderegg, G.; Hubmann, E.; Podder, N. G.; Wenk, F. *Helv. Chim. Acta* **1977**, *60*, 123–140.
(32) Kagi, J. H.; Vallee, B. L. *J. Biol. Chem.* **1961**, *236*, 2435–42.
(33) Petering, D. H.; Zhu, J.; Krezoski, S.; Meeusen, J.; Kiekenbush, C.; Krull, S.; Specher, T.; Dughish, M. *Exp. Biol. Med.* **2006**, *231*, 1528–34.
(34) Rana, U.; Kothinti, R.; Meeusen, J.; Tabatabai, N. M.; Krezoski, S.; Petering, D. H. *J. Inorg. Biochem.* **2008**, *102*, 489–99.
(35) Namdarghanbari, M. A.; Meeusen, J.; Bachowski, G.; Giebel, N.; Johnson, J.; Petering, D. H. *J. Inorg. Biochem.* **2009**, *104*, 224–31.
(36) Lindskog, S.; Malmstrom, B. G. *J. Biol. Chem.* **1962**, *237*, 1129–37.
(37) Strandberg, B.; Tilander, B.; Fridborg, K.; Lindskog, S.; Nyman, P. O. *J. Mol. Biol.* **1962**, *5*, 583–4.
(38) Hurst, T. K.; Wang, D.; Thompson, R. B.; Fierke, C. A. *Biochim. Biophys. Acta* **2010**, *1804*, 393–403.
(39) Jindal, R. M.; Gray, D. W.; McShane, P.; Morris, P. J. *Biotech. Histochem.* **1993**, *68*, 196–205.
(40) Andrews, J. C.; Nolan, J. P.; Hammerstedt, R. H.; Bavister, B. D. *Cytometry* **1995**, *21*, 153–9.
(41) Frederickson, C. J.; Cuajungco, M. P.; LaBuda, C. J.; Suh, S. W. *Neuroscience* **2002**, *115*, 471–4.
(42) Frederickson, C. J.; Rampy, B. A.; Reamy-Rampy, S.; Howell, G. A. *J. Chem. Neuroanat.* **1992**, *5*, 521–30.
(43) Fu, Y.; Tian, W.; Pratt, E. B.; Dirling, L. B.; Shyng, S. L.; Meshul, C. K.; Cohen, D. M. *PLoS One* **2009**, *4*, e5679.
(44) Kitamura, Y.; Iida, Y.; Abe, J.; Mifune, M.; Kasuya, F.; Ohta, M.; Igarashi, K.; Saito, Y.; Saji, H. *Biol. Pharm. Bull.* **2006**, *29*, 821–3.
(45) Kothinti, R.; Blodgett, A.; Tabatabai, N. M.; Petering, D. H. *Chem. Res. Toxicol.* **2010**, *23*, 405–12.
(46) Heuchel, R.; Radtke, F.; Georgiev, O.; Stark, G.; Aguet, M.; Schaffner, W. *EMBO J.* **1994**, *13*, 2870–5.
(47) Andrews, G. K. *BioMetals* **2001**, *14*, 223–37.
(48) Wimmer, U.; Wang, Y.; Georgiev, O.; Schaffner, W. *Nucl. Acid. Res.* **2005**, *33*, 5715–27.
(49) Krezel, A.; Maret, W. *J. Biol. Inorg. Chem.* **2006**, *11*, 1049–62.
(50) Vinkenborg, J. L.; Nicolson, T. J.; Bellomo, E. A.; Koay, M. S.; Rutter, G. A.; Merkx, M. *Nat. Methods* **2009**, *6*, 737–40.
(51) Ling, H.; Vamvakas, S.; Schaefer, L.; Schnittler, H. J.; Schaefer, R. M.; Heidland, A. *Nephrol., Dial., Transplant* **1995**, *10*, 1305–12.
(52) Paski, S. C.; Covery, L.; Kummer, A.; Xu, Z. *Can. J. Physiol. Pharmacol.* **2003**, *81*, 815–24.
(53) Krezel, A.; Maret, W. *J. Am. Chem. Soc.* **2007**, *129*, 10911–21.
(54) Coyle, P.; Zalewski, P. D.; Philcox, J. C.; Forbes, I. J.; Ward, A. D.; Lincoln, S. F.; Mahadevan, I.; Rofe, A. M. *Biochem. J.* **1994**, *303*, 781–6.